Fermilab

TM-1424
0427.110
(SSC-N-242)

The 5cm Aperture Dipole Studies*

A.D. McInturff, R. Bossert, J. Carson, H.E. Fisk, R. Hanft,
M. Kuchnir, R. Lundy, P. Mantsch, and J. Strait

September 30, 1986

*Submitted to the 1986 Applied Superconductivity Conference,
Baltimore, Maryland, September 28 - October 3, 1986

THE 5cm APERTURE DIPOLE STUDIES

A.D. McInturff, R. Bossert, J. Carson, H.E. Fisk,
R. Hanft, M. Kuchnir, R. Lundy, P. Mantsch, and J. Strait
Fermi National Accelerator Laboratory*
P.O. Box 500
Batavia, Illinois 60510

Abstract

The results obtained during the evolution of the design, construction, and testing program of the design "B" dipole, are presented here. Design "B" is one of the original three competing designs for the Superconducting Super Collider[1] "SSC" arc dipoles. The latest design "B" cross-section is shown in Fig. 1. The final design parameters were as follows: air cored (less than a few percent of the magnetic field derived from any iron present), aluminum collared, two layered winding, 5.5T maximum operating field, and a 5cm cold aperture. There have been fourteen 64cm long 5cm aperture model dipoles cold tested (at 4.3K and less) in this program so far. There was a half length full size (6m) mechanical analog (M-10) built and tested to check the cryostat's mechanical design under ramping and quench conditions.[2] Several deviations from the 'Tevatron' dipole fabrication technique were incorporated, for example the use of aluminum collars instead of stainless steel. The winding technique variations explored were "dry winding,"[3] a technique with the cable covered with Kapton insulation only and "wet winding" where the Kapton was covered with a light coat of "B" stage epoxy. Test data include quench currents, field quality (Fourier multipole co-efficients), coil magnetization, conductor current performance, and coil loading. Quench current, loss per cycle, and harmonics were measured as a function of the magnitude and rate of change of the magnetic field, and helium bath temperature.

Introduction

The cold (≤4.3K) testing of these early prototypes (SB1001 and SC1001) was conducted without their cold iron shields. One of the features of the latest design of the "SSC" dipoles is a cold iron shield. The first two prototypes were "iron core" (greater than ten percent of the magnetic field derived from the iron present) designs. Both designs included a cold iron shield. After examining various cool down scenarios for the machine, it was decided to optimize the air core version of the 5cm dipole. This version had a definite advantage in the refrigeration cooldown and warmup cycle time due to the reduced cold mass. The first air core prototype was constructed from an existing cable whose material was readily available even though the dimensions would not result in the proper magnetic field shape, SF1001. It was primarily a winding exercise and quench performance check (See Tabs. 1 and 2). The next series of prototypes used a thick wedge, (i.e., the inner radius azmuthal thickness of the wedge was non zero), SG100X. These magnets performed well, but had the wrong turn distribution as well. Then a series of prototypes with the proper turn distribution were fabricated; SJ100X for the dry wound series, and SK100X for the wet wound series. The magnetic field shapes for those series were not as good as had been anticipated based on careful magnetic field calculations (although they were consistent within a group). The problem was finally traced to the collaring method and excessive preload. There were actually 22 collared coil assemblies made, but only 14 were cold tested. The magnets that were cold tested had their quench history and magnetic field quality in the central region measured and recorded. Their "Energy(In) minus Energy(Out)" profiles were measured as a function of current and rate of change of magnetic field. There was a subset of these collared coils which had strain gauges mounted in them. Measurements of the load on the collar were made using these strain gauges. These measurements include data from before closing the collars to closure of the collars and then relaxing at room temperature. The strain gauges were temperature

Table 1. 5cm Aperture Model Parameters

Strand Type Cu/Sc Fil Ratio dia (μ)	Winding Type Dry	Wet	No of Cable Strands Inner / Outer	Cable Short Sample ρeff 2×10^{-12} Ω-cm 4.2K Field (T)	Inter Layer Banding Kapton H O L E	S O L I D	Collar Lam SS	Al	Strand Insul Z S E T B A R B A R I T E
SB1001 1.8 9		X	23/23	4600/5	X		X*		X
SC1002 1.8 9	X		23/23	5328/5		X		X*	X
SF1001 1.6 20	X		25/23	8650/6		X		X	X
SG1003 1.7 17	X		25/23	7870/6		X		X	X
SG100N 1.7 17	X		25/23	7870/6	X			X	X
SG1006 1.8 17	X		25/23	7870/6		X		X	X
SJ1003 1.8 17	X		25/23	7870/6		X		X	X
SJ1006 1.8 17	X		25/23	7720/6		X		X	X
SJ1008 1.8 17	X		25/23	7720/6		X		X	X
SJ1009 1.8 17		X	25/23	7720/6		X		X	X
SJ1010 1.8 17	X		25/23	7720/6		X		X	X
SK1001 1.8 17		X	25/23	7870/6		X		X	X
SK1002 1.8 17		X	25/23	7870/6		X		X	X
SK1003 1.8 17		X	25/23	7720/6		X		X	X

*Solid, not laminated

*Operated by Universities Research Association, Inc., under contract with the U.S. Department of Energy.

Manuscript received September 30, 1986.

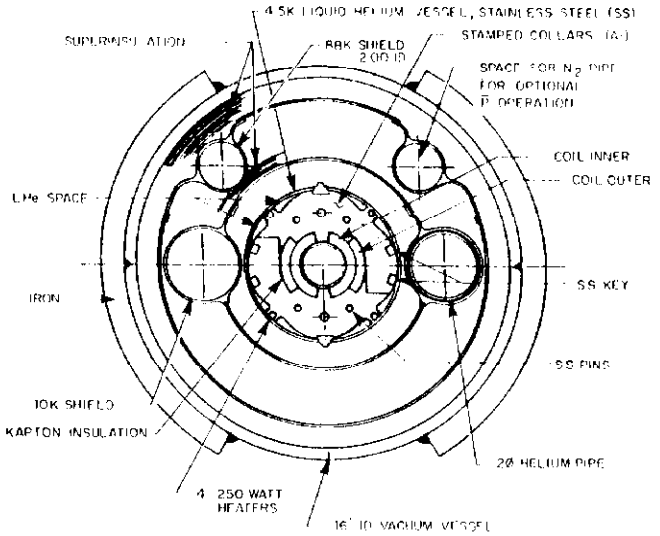

Figure 1: Detailed cross section of the 5.5T, 5cm aperture reference Design B dipole magnet. The cold aperture is 5.1cm in diameter.

Table 2. Performance

Design Current with Fe or As Design w/o Fe As Built	Design Field (T) Same as Current	First Quench Short Sample	Maximum Current 4.2K	Trans Funct Gauss/Amp	Co-efficients B_1/A_1 1/cm x 10^4	B_2/A_2 $1/cm^2$
SB1001						
4125	5.0	4300	4750	8.00		-18.0
4850	4.0	5150				0.0
SC1002						
4125	5.0	4800	5750	8.06	3.1	6.2
4850	4.0	5675			1.0	0.6
SF1001						
5800	5.0	780	7305	7.3	-3.1	30.0
6800	5.0	7770			0.5	-0.2
SG1003						
5800	5.0	6070	7330	8.22	4.5	42.5
6050	5.0	7160			1.0	-0.2
SG1004						
5800	5.0	6050	7210	8.22	-3.0	42.0
6050	5.0	7160			0.5	0.5
SG1006						
5800	5.0	5580	7080	8.22	-1.0	48.0
6050	5.0	7160			-1.0	1.9
SJ1003						
5800	5.0	5500	7150	8.36	-0.1	7.2
5900	5.0	6975			-1.6	0.7
SJ1006						
5800	5.0	5390	6785	8.31	-0.7	11.3
5900	5.0	6830			4.5	-0.8
SJ1008						
5800	5.0	5205	7174	8.31	1.2	7.7
5900	5.0				4.2	-0.2
SJ1009						
6390	5.5	5954	7075	8.31	1.0	11.3
6490	5.5	6830			1.8	-0.4
SJ1010						
6390	5.5	5703	7031	8.31	1.0	11.6
6490	5.5	6830			-2.0	-0.1
SK1001						
5800	5.0	4990	7080	8.31	-3.0	16.1
5900	5.0	6975			0.0	2.2
SK1002						
6390	5.5	6015	6985	8.31	-1.0	13.7
6490	5.5	6975			9.0	1.6
SK1003*						
6390	5.5	5623	6390	8.31	-0.4	9.1
6490	5.5	6830*			-0.6	-0.4

* 1 Wire Missing

compensated so data were taken during cool down to 4.2K and during the magnet powering sequence. All of these coils ran at reduced temperature, most at 3.2K, during some period of their training cycle. During the prototype construction period, the critical current density of NbTi improved almost 35%. Due to the higher critical current of the magnet conductor, the magnet performance exceeded the original design goals of 5.0T. It was decided to increase the operating field to 5.5T. If present higher performance conductor were used, the operating field would be 6.0T.

Experimental Procedure

The standard magnet test procedure was to verify the high voltage integrity of the coil after it was vertically mounted in the test fixture. The continuity of the voltage taps and the strain gauges were measured and checked against the values attained after collaring of the winding. These measurements were repeated during and after the cooldown of the magnet to 4.2K. The quench performance of the magnet was measured. The Energy(In) minus Energy(Out) profile was measured for both a 3.32 and a 5.4 Tesla cycle as a function of ramp rate. The magnet was then subcooled by .5 - 1 degree Kelvin and repeatedly quenched until it quenched at the same current each time it was energized or became random. The magnet was then warmed to 4.2K. The quench current of the magnet was measured as a function of rate of change of magnetic field. A warm re-entrant bore tube containing a "Morgan coil"[4] was then mounted in the aperture. The harmonics were measured; first the DC harmonics and then later the ramped harmonics. Special studies of the time variation of harmonics, i.e., the fast and slow change of the sextupole term given various magnet powering cycles, were made. A Rawson probe was used to measure the longitudinal shape of the field. In certain circumstances, the magnet temperature was lowered and the harmonic measurements were repeated as a function of temperature.

Results and Conclusions

Quench Performance

The quench history is given for a typical magnet in this series and for the best in Fig. 2. The quench

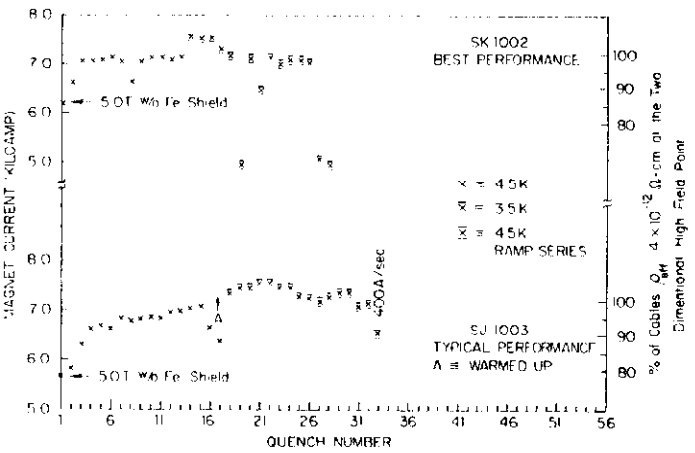

Figure 2: The quench current is plotted as a function of quench number for the best quench performance, SK1002, and the average, SJ1003.

current performance can be expressed as a percent of the intersection of the cable's effective resistivity (2×10^{-12} Ω-cm) curve and the winding highest two dimensional field load line. The cable's resistivity is measured with it's wide surface perpendicular to

the magnetic field. It took the typical coil about six quenches to reach 95% while the best performance was three. The coil SK1002 had achieved 99%+ on the third quench. The typical coil had to be quenched at reduced temperature to reach 99%+ or else ten to twenty times at 4.2K.

Collar Preload

The stress on the coil as measured by strain gauges in the collars is shown in Fig. 3. It is clear that the maximum strain on the collared coil package occurs during the closure of the collars. The peak stress occurs when the keys are slipped into the slots in the collars that lock the collars together. This stress is almost twice (1.93) that of the residual stress left in the collared coil package after two weeks at room temperature. Each collar lamination was connected to its neighbor via two stainless steel pins. The pins couple adjacent laminations mechanically (see Fig. 1). The tolerances necessary to enable assembly also allow the right and left laminations to move with respect to one another. When the collars are being clamped on the windings by the press, this hinge motion allows the coil to expand in the "x" axis (midplane). Once the keys are in place and the press removed the coil loading reverses this hinged motion allowing the collared coil to expand in the "y" axis (polar). A solution proposed for this problem is to spot weld right and left pairs[5] at the pin positions.

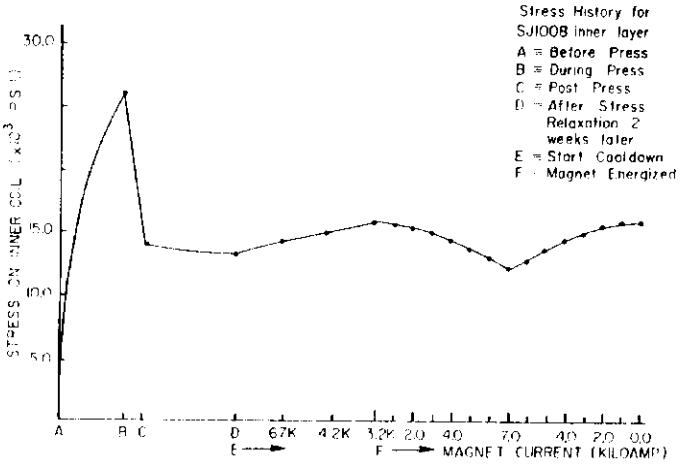

Figure 3: This is a graphical history of a 'dry winding' collared coil, SJ1008 from the time it was placed in the collaring press through the low temperature power cycling of the coil to 5.8T and back to 0T. Note the magnitude of the stress during the initial closing of the collars.

The advantage of the aluminum collars is illustrated in Figure 3. Seventy-one percent of the pre-stress needed for the magnetic field load is supplied by the difference in contraction of the aluminum collars ($\int_{4.2K} \Delta L/L = 4.5 \times 10^{-3}$) versus the coil package ($\int_{4.2K} \Delta L/L = 3 \times 10^{-3}$). This collar design employed keys to lock it into place. The effect of the magnetic field loading is only about 20% of the peak stress seen by the coil or 28% of the residual room temperature stress after collaring and being keyed.

Helium Irrigation

The amount of helium irrigation in these coils was minimum for the dry windings to practically zero for the wet windings. The void volume in the windings that helium can occupy is only a few percent. This was not considered to be a problem because the cycle time for the "SSC" was very long, requiring only a 50 gauss/second ramp rate. If helium circulation were a problem, then the quench current should be very ramp rate sensitive. The data are shown in Fig. 4. In the worst case, only about a 10% reduction in the quench current for ramp rates from 25 gauss/second up to 1660 gauss/second occurs.

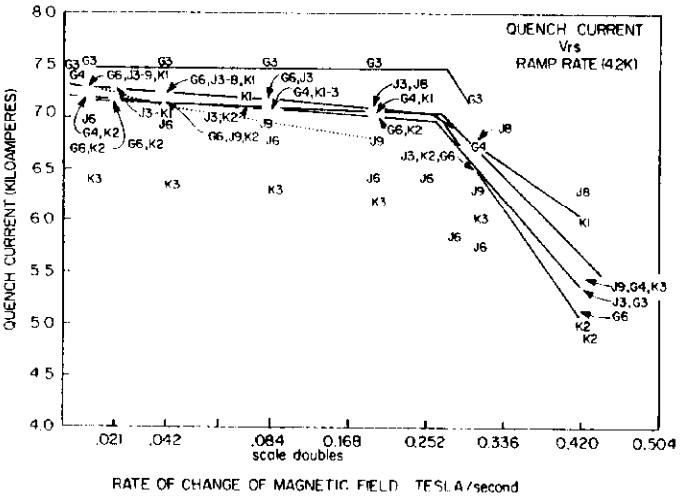

Figure 4: This is a graph of the quench current for the various models as a function of the rate of change of magnetic field. Note in the area of interest ≈ 50 gauss/sec, the quench current is very insensitive. The symbol "K2" stands for the collared coil assembly SK1002, K1 = SK1001, J3 = SJ1003, etc.

Energy Loss and Coil Magnetization

Fig. 5 is typical data of Energy(In) minus Energy(Out)[6] for the prototype "SJ1010". The loss per cycle for a full scale 12m collared coil assembly would be ~ 338 ± 36 joules for the 17μ filament conductor used in these prototypes. The loss/cycle of these prototypes increased about 20% by increasing the ramp rate a factor of three times that proposed for the SSC as shown in Fig. 6. This value would be reduced by a factor of four to eight in the actual

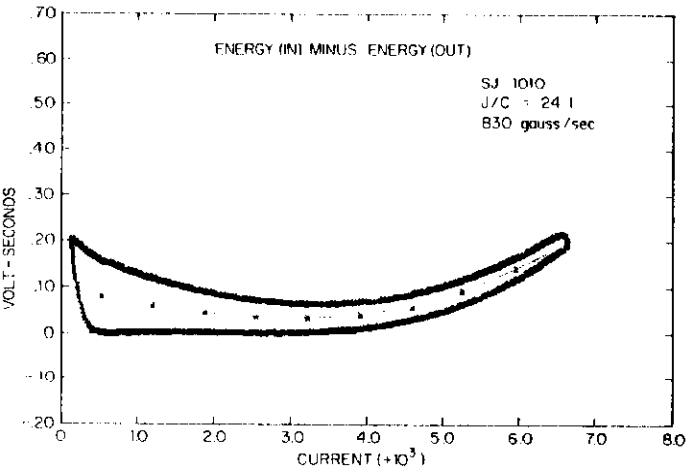

Figure 5: This is a graph of the data of the Energy(In) minus Energy(Out) as measurement as plotted by the computer.

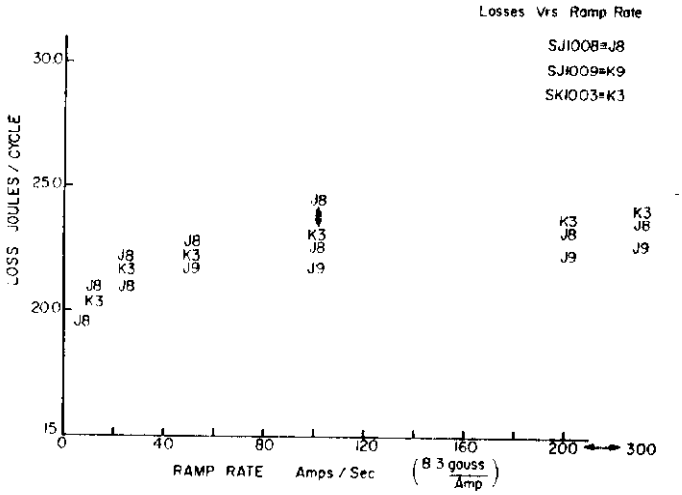

Figure 6: The loss/cycle of the 'B' series dipoles as a function of rate of change of magnetic field is shown above. The losses only increases about 20% for ramp rates up to two to three times that of the proposed SSC cycle.

magnets due to the additional requirement to minimize the magnetization effects of the sextupole harmonic width. A filament size of 2 to 4 microns is required in order not to need to correct the field shape.

The shape of the Energy(In) minus Energy(Out) curve $\sim C\ (I-I_o)^2$ is to some extent a measure of how stiff the winding and supporting structure are[7]. Tab. 3 lists the constants of this imperical equation when fitted to the E-(in) minus E-(out) profiles. Smaller values indicate stiffer coils, i.e., smaller change in inductance per unit of Lorentz force. With the exception of SF1001, all of the coils wound without the fiberglass tape were stiffer, SC and on, versus the R series magnets that use B stage fiberglass. The value of "C" ranged from 0.08 to 0.14 volt-sec/kA^2 for the R series.[8]

Table 3. Shape of E(in)-E(out) Curves $\sim C(I-I_o)^2$

Model	C(Volt-sec)/kA^2	I_o(kA)
SB 1001	0.022 ±.004	0.55
SC 1002	0.017 ±.004	0.55
SF 1001	0.040 ±.004	1.0
SG 1003	0.011 ±.003	0.75
SG 1004, 6	0.013 ±.003	1.6
SJ 1003	0.019 ±.002	1.6
SJ 1006	0.015 ±.002	1.6
SJ 1008	0.011 ±.002	1.6
SJ 1009	0.008 ±.002	1.6
SJ 1010	0.010 ±.002	1.6
SK 1001	0.009 ±.002	1.6
SK 1002	0.011 ±.002	1.6
SK 1003	0.015 ±.002	1.6

Magnetic Field Characteristics

A set of Fourier co-efficients measured at 5.0T central field are given in Tab. 4 for the correct turn distribution prototypes. It is of interest here to note that the sextupole and decapole terms were designed to be zero for the models SJ100X and SK100X, actually were in fact, ~ 10 and 1.5×10^{-4} at one centimeter respectively. It has been calculated that an ellipticity of 0.635mm in the polar direction of the magnet would account for these values and this solution was relatively easy to check by measuring the midplane diameter versus the polar diameter of the collared coil package. The diameter measurements were in agreement. This ellipticity was traced back to both the excessive preload and the collaring process. Figs. 7 and 8 show the 'in phase and out of phase' sextupole (B_2 and A_2) and decapole (B_4 and A_4) curves as a function of coil current respectively. Note the large difference in sextupole values on the up ramp versus the down ramp ~ 7.5 unit ($\times 10^{-4}$) at 0.84T.

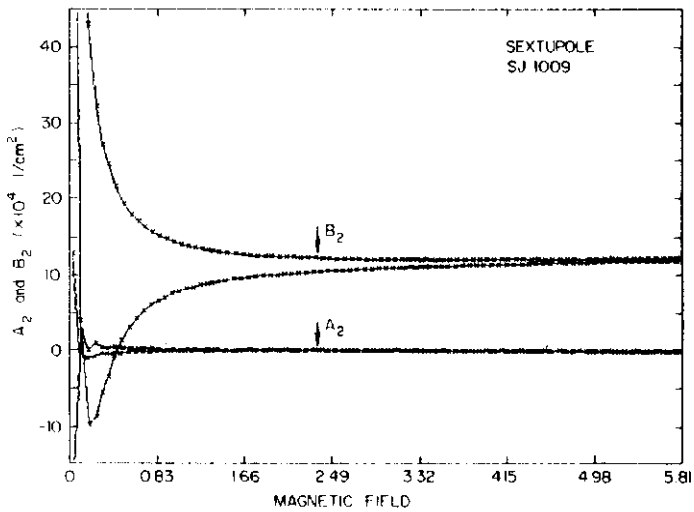

Figure 7: The sextupole in-phase 'B_2' and out of phase 'A_2' measured Fourier co-efficients for SJ1009 are plotted as a function of magnetic field.

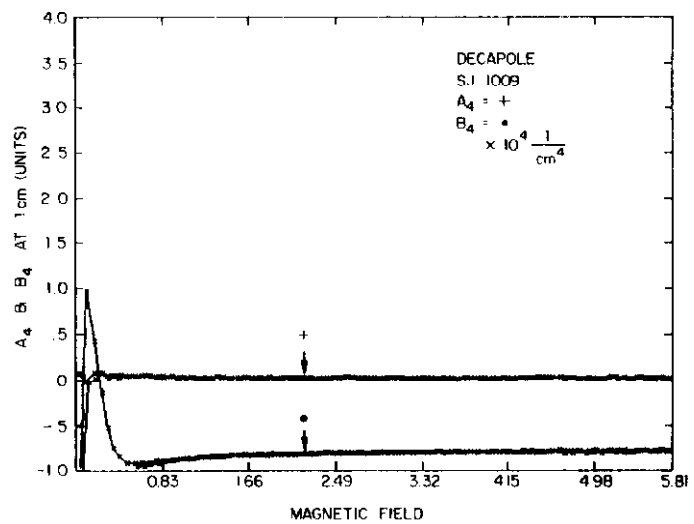

Figure 8: The decapole in-phase 'B_4' and out of phase 'A_4' measured Fourier co-efficients for SJ1009 are plotted as a function of magnetic field.

The proposed injection field is 0.84T. A value less than a unit or two will be required in order not to be corrected at injection. The ramp cycle magnetization effects of the sextupole term were investigated due to an apparent change in chromaticity of the beam during the 'Tevatron' injection cycle in the collider operation mode. A long time (many minutes) and short term (a few seconds or fractions of) change of the sextupole field was measured during these powering sequences, and therefore accounted for the beam behavior.

The longitudinal profile of the magnetic field in

the short models was measured. The magnetic length was found to be 68.38cm as shown in Fig. 9. The 'Morgan' coil probe was located at the center of the magnet and was 38.1cm long; therefore, the effect of the model magnet ends should not be present in the harmonic co-efficients measured and presented in Tab. 4.

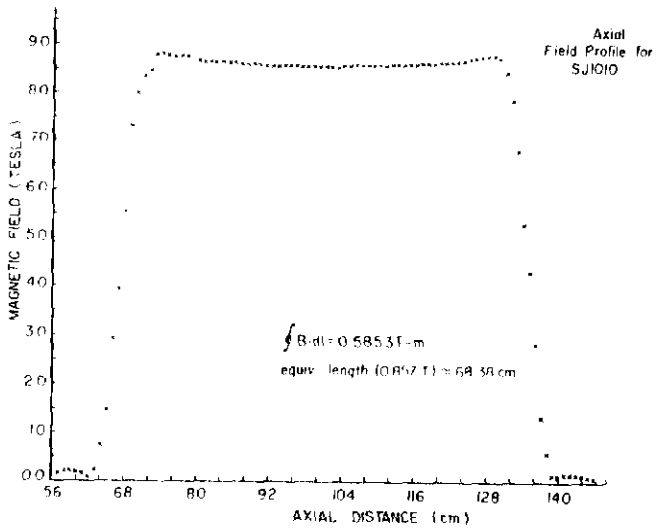

Figure 9: This is the axial profile of the magnetic field as measured with a Rawson probe. Note the magnetic length of the magnet is 68.38cm or the bending power is H(0,0) middle of magnet times 0.6838 = 0.5853T-m.

Table 4. Measured Fourier Co-Efficients x 10^4 $1/cm^n$

	A_1	B_1	A_2	B_2	A_3	B_3	A_4	B_4
SJ 1003	-1.6	-0.1	0.7	7.2	0.6	-0.7	0.2	-0.3
SJ 1006	4.5	-0.7	-0.8	11.3	-0.4	-0.3	-0.1	1.0
SJ 1008	4.2	1.2	-0.2	7.7	0.0	-0.1	-0.1	0.9
SJ 1009	1.8	1.0	-0.4	11.3	0.1	-0.2	0.0	0.7
SJ 1010	-2.0	1.0	-0.1	11.6	0.6	0.1	-0.0	-0.6
SK 1001	0.0	-3.0	2.2	16.1	0.2	0.4	-0.2	1.7
SK 1002	9.0	-1.0	1.6	13.7	-1.7	-0.1	-0.1	1.5
SK 1003	-0.6	-0.7	-0.4	9.1	0.3	-0.6	-0.0	1.0

The transfer constant measured at 6000 Amperes for a typical prototype was 8.28 ±.04 gauss/ampere. Note in the actual ring magnet due to the iron vacuum shell, the transfer constant value would be ≈ 3% higher.

Conclusions

The questions investigated and answers found by this dipole prototype study were:

1. Is the design "B" iron free magnet a viable arc dipole for the SSC accelerator? The answer is yes. The magnetic field quality is reproducible, and seems to be well understood. The construction technique will control the harmonics to within a unit ($x10^{-4}$ $1/cm^n$) of the desired value. The operating magnetic field range of 5.5T to 6.0T, which has been demonstrated for the design "B" magnet, is certainly acceptable for the SSC.

2. Is the 'dry winding' technique viable as a production method? This question is answered in detail in a companion paper by "Carson and Bossert"[3] at this Conference, and by the magnet performance reported here. After a period of development, several collared coils were successfully assembled and tested. The performance problems with the magnets, when they occurred, were normally fixed by tightening or reworking the ends of the coils. The production cost savings are obvious due to the absence of the curing steps. Therefore, additional development to further perfect this technique should be pursued.

3. Is the 'wet winding' technique using "B" staged epoxy coated Kapton only rather than the combination of "B" staged fiberglass and Kapton, viable as a production method? The answer to this question is yes, as well. This particular fabrication technique, although it did not remove the curing step, produced higher density windings than fiberglass insulated ones. These higher density windings, of course, were capable of producing a higher magnetic field for a given winding volume.[8] The best quench history of this study was a collared coil produced by this technique, SK1002.

4. Is aluminum a suitable collar material? The data shown in Fig. 3 clearly shows one of the best features of aluminum, namely the reduction of the preload needed to offset the magnetic load. This reduction can be as high as 70%, as was the case in SJ1008. The performance of the aluminum collared coils have been as good or better than their stainless steel counterparts.[8]

References

1. M. Tigner, 'Superconducting Super Collider' Reference Design Study for U. S. Department of Energy, Report of the Reference Designs Study Group, May 8, 1984.

2. P. Mazer, J. Carson, N. Engler, H. Fisk, J. Gonczy, R. Hanft, M. Kuchnir, P. Mantsch, A. D. McInturff, T. Nicol, R. Niemann, E. Schmidt, and A. Szymulanski, "5cm No Iron SSC 6m Dipole Test Program," CEC/ICMC Conference, Boston, Ma., August, 1985.

3. J. Carson and R. Bossert, "A Technique for Epoxy Free Winding and Assembly of Cos H Coils for Accelerator Magnets," presented in this Conference.

4. G. H. Morgan, "Stationary Coil for Measuring the Harmonics in Pulsed Transport Magnets," Proc 4th Int'l. Conf. on Magnet Technology, Brookhaven, Sept 19-22, 1972, Y. Winterbottom, Ed., USAEC Conf-720908, NTIS, Springfield, Va., 22151 (1973), pgs. 787-790, BNL #17190.

5. C. Goodzeit, BNL Private Communication

6. M. N. Wilson, CRYOGENICS, June, 1973, pg. 361.

7. A. D. McInturff and D. Gross, IEEE TRANSACTIONS on Nuclear Science, Vol NS-28, No. 3, pg. 3211, June, 1981.

8. A. D. McInturff, J. Carson, N. Engler, H. Fisk, R. Hanft, R. Lundy, P. Mantsch, T. Nicol, R. Niemann, E. Schmidt, and A. Szymulanski, IEEE TRANSACTIONS on Magnetics, Vol. MAG-21, No. 2, pg. 478, March, 1985.